Journal of Solid State Chemistry 181 (2008) 2748–2754

Contents lists available at ScienceDirect

Journal of Solid State Chemistry

journal homepage: www.elsevier.com/locate/jssc

Al_2O_3 @ TiO_2—A simple sol–gel strategy to the synthesis of low temperature sintered alumina–aluminium titanate composites through a core–shell approach

M. Jayasankar [a], S. Ananthakumar [a], P. Mukundan [a], W. Wunderlich [b], K.G.K. Warrier [a,*]

[a] Materials and Minerals Division, National Institute for Interdisciplinary Science and Technology (NIIST) (Formerly Regional Research Laboratory (CSIR)), Thiruvananthapuram, India

[b] Faculty of Engineering, Department of Material Science, Tokai University, Kanagawa 259-1292, Japan

ARTICLE INFO

Article history:
Received 22 January 2008
Received in revised form
26 June 2008
Accepted 30 June 2008
Available online 15 July 2008

Keywords:
Sol–gel
Grain size
Nanocomposite

ABSTRACT

A simple sol–gel based core–shell approach for the synthesis of alumina–aluminium titanate composite is reported. Alumina is the core and titania is the shell. The coating of titania has been performed in aqueous medium on alumina particle by means of heterocoagulation of titanyl chloride. Further heat treatment results in low temperature formation of aluminium titanate as well as low temperature sintering of alumina–aluminium titanate composites. The lowering of the reaction temperature can be attributed to the maximisation of the contact surface between the reactants due to the core–shell approach involving nanoparticles. The mechanism of formation of aluminium titanate and the observations on densification features in the present process are compared with that of mixture of oxides under identical conditions. The sintered alumina–aluminium titanate composite has an average grain size of 2 μm.

1. Introduction

Aluminium titanate has drawn much attention as a high temperature material due to the low thermal expansion coefficient [1] and high thermal shock resistance [2]. Aluminium titanate exhibits two allotropic forms such as α and β, where β aluminium titanate is the low temperature stable phase [3]. Aluminium titanate is usually formed by the solid-state reaction between alumina and titania above the eutectoid temperature 1280 °C [4]. Aluminium titanate exhibits microcracking during cooling from the sintering temperature due to the thermal expansion anisotropy [5]. Microcracks are found to develop predominantly above a critical sintered grain size of 1.5 μm and therefore fine-grained microstructure is necessary. The excellent properties like thermal shock resistance and low thermal conductivity coupled with good chemical resistance to molten metals (particularly aluminium) result in the aluminium titanate fulfilling several metal contact applications in the foundry industry [6].

Alumina is a known ceramic material because of its high temperature stability, chemical inertness and wear resistance. However, alumina lacks thermal shock resistance and has a relatively high thermal expansion coefficient of $8.7 \times 10^{-6}\,^{\circ}C^{-1}$ [7]. Earlier reports indicate that addition of higher quantity of aluminium titanate particles of uniform size would improve the thermo-mechanical response of the composite. The alumina–aluminium titanate composites exhibit functional as well as structural properties for application as thermal barrier coating, insulating components for diesel engines and high temperature substrate. Padture et al. reported that alumina–aluminium titanate composite with a uniform distribution of alumina particles results in excellent flaw tolerance [8]. Different techniques are adopted for the fabrication of alumina–aluminium titanate composite. The aims of different techniques are to reduce the formation temperature of aluminium titanate [9] as well as to avoid microcracking due to the thermal expansion anisotropy of aluminium titanate. To the best of our knowledge, no attempt has been made to synthesise aluminium titanate in alumina matrix through a simple sol–gel core–shell approach, which is shown to have advantage with respect to controlled fine grain size and homogeneity of distribution of phases.

Over the last decade, there have been immense efforts to fabricate core–shell materials with tailored structural, optical, and surface properties [10]. The main application of nanocoated particles may either be seen in the formation of diffusion barriers to avoid grain growth or in the modification of physical properties of the core and the chemical properties of the surface [11]. Techniques similar to core–shell approach were reported for

* Corresponding author. Fax: +91 471 491712.
E-mail address: wwarrierkgk@yahoo.co.in (K.G.K. Warrier).

0022-4596/$ - see front matter © 2008 Elsevier Inc. All rights reserved.
doi:10.1016/j.jssc.2008.06.057

preparing powder having a uniform coating of $BaTiO_3$ on Ni particles. The reduction in shrinkage rate is achieved by preventing Ni from oxidation during sintering, which makes it useful as a multilayer ceramic capacitor [12]. Monodisperse silica spheres with magnetic cores were formed by silica precipitation on to magnetite particles [13]. Titania-coated silica spheres have received a lot of attention because of their potential use in catalytic, pigment, and photonic crystal application [14]. Micrometre-sized iron particles were coated with silica by the hydrolysis of TEOS in order to improve the oxidation behaviour of iron particles [15]. Recently, boehmite coating on Si_3N_4 was found to improve the consolidation density as well as the green-state plasticity of Si_3N_4. Therefore, the ceramic coating not only can improve the distribution of sintering aids, but also modify the rheological and consolidation behaviour of a ceramic suspension [16]. Microcomposite particle consisting of alumina core and amorphous silica coating to form mullite phase is reported in which full densification is achieved at as low as 1300 °C. The problem of heterogeneity of the second constituent in the preparation of ceramics can be considerably solved by the core–shell approach.

Here, we report a simple and effective sol–gel method through core–shell approach for the synthesis of alumina–aluminium titanate composite. This method is effective in controlling the grain size of alumina and aluminium titanate, low temperature formation of aluminium titanate and further low temperature sintering of the composite.

2. Experimental

2.1. Materials

Titanium tetrachloride (99% purity, M/S Kerala Minerals and Metals Ltd., Kollam, India), A16 SG alumina powder (99% purity, ACC-ALCOA Chemicals, Kolkata, India, average particle size 0.3 μm), HNO_3 (Merck, India) solution, and ammonia solution 25% (S.D. Fine Chemicals, India) were used.

2.2. Preparation of titania sol

In a typical experiment, to prepare the titania sol, titanium tetra chloride was dissolved in ice cold distilled water (0.2 M) and was hydrolysed by slow addition of ammonium hydroxide (25% S.D. Fine Chemicals, India), solution under constant stirring at room temperature, until the reaction mixture attained pH 9.0. The precipitate was separated by filtration and was washed free of chloride ions (as was confirmed by the AgCl test) with hot distilled water. The precipitate (5 g) was further dispersed in 1000 mL water and was peptised by the addition of 20% HNO_3 (Merck, India) solution [17].

2.3. Titania coating over alumina particle

The estimated titania sol was used to coat on alumina kept in suspension, which was prepared by dispersing alumina powder (depending on the respective compositions) in 1000 mL of water. Stirring was continued for 30 min and the additional titania required for aluminium titanate was added in the form of titanium hydroxide precipitate (depending on the required compositions). The whole mixture was then peptised to a stable suspension by the addition of 20% HNO_3 (Merck, India) which was flocculated by slow addition of ammonium hydroxide to bring to pH 6.5 and was further dried in an oven at 80 °C [18].

2.4. Characterisation of titania coating over alumina particle

Zeta potential was measured using a Zetasizer Malvern Instrument UK. Small amounts of Al_2O_3, TiO_2, and Al_2O_3 @ TiO_2 powder were separately dispersed in water and the pH was adjusted using 0.1 M HNO_3 or NaOH for acidic and basic solutions, respectively. The final zeta potential was the mean value averaged from three measurements.

The particle size analysis was carried out using laser particle size analyser on the powders calcined at 80 and 1000 °C (Zeta Sizer, Malvern Instruments, UK). The sample for the particle size analysis was made by ultrasonic dispersion of the respective powders (1 g) in aqueous medium (100 mL) at pH < 2.0. Average of three measurements with in a standard deviation of 3.0% is reported.

The coating of titania on alumina particle was observed under transmission electron microscope (FEI, TECNAI 30 S-Twin (the Netherlands)) operated at 300 kV and equipped with an energy-dispersive X-ray analyser (EDX). The powder was dispersed in acetone and a drop of the suspension was deposited on a carbon-coated copper grid (TEM) and dried.

X-ray photoelectron spectroscopy (XPS) was performed using a Quantum 2000 device by Ulvac-Phi, Japan, on the composite precursor sample calcined at 1000 °C.

The dried precursor gels were subjected to DTA analysis (Shimadzu, DTA-50 H) at a heating rate of 5 °C min^{-1} up to 1400 °C. The dried gels were individually heated at 1350 °C in electric muffle furnace and then cooled in air to room temperature. The phase identification was done using XRD (Philips PW 1170) in the 2θ range of 20–60 Cu$K\alpha$. The structure evolution was done by the FTIR analysis.

The precursor was calcined at 900 °C compacted uniaxially at 200 MPa using 2 wt% PVA as binder and sintered in the range 1350–1450 °C. Morphological characterisation of the sintered pellet was performed using scanning electron micrograph (SEM, JEOL, JSM 560 LV, Japan) on samples after polishing and thermally etching at 1325 °C. The average grain size was calculated by the linear intercept method using the relation $G = 1.5L/MN$ where 1.5 is a geometry dependent proportionality constant, L is the total test line length, M the magnification and N the total number of intercepts. For the grain size determination, four representative micrographs with the magnification of 4000 × were analysed. A test line of 9 cm length was marked on the micrograph and the number of intersections of the line with grain boundaries was counted.

2.5. Preparation of a reference sample

In order to compare the reactivity of the titania-coated alumina particles as well as the properties of final alumina–aluminium titanate powders with the conventional solid-state process, a mixture of the same alumina powder used for the coating process and TiO_2 (anatase TiO_2, Sigma-Aldrich) was prepared by ball milling in water. The powder was subjected to similar thermal treatment as that of the coated precursor.

3. Results and discussion

3.1. TiO_2-coated Al_2O_3 particle

Zeta potential of the alumina, titania, and the titania coated alumina were measured with Malven Zeta sizer. The results are shown in Fig. 1. The isoelectric point of alumina was located at the pH 7.8 which has shifted to 4.5 after coating with titania. Study

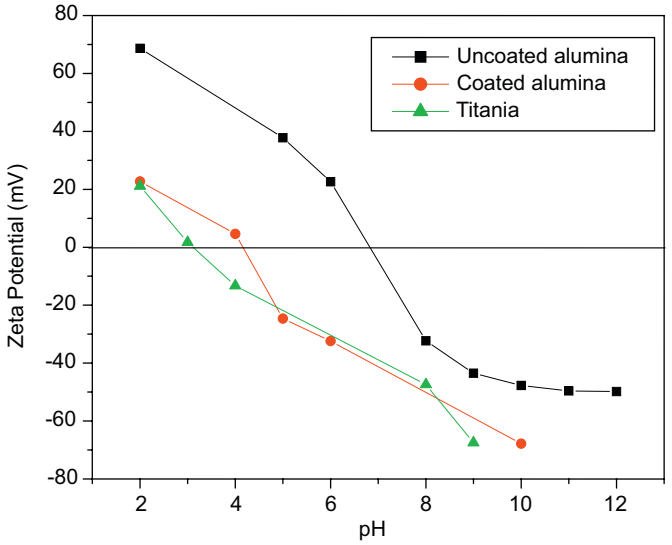

Fig. 1. Zeta potential measurement of alumina, titania, and titania coated alumina particle.

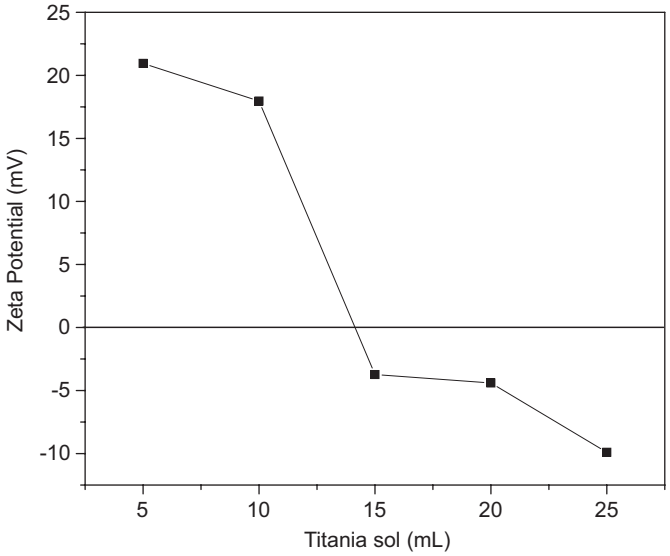

Fig. 2. Variation in zeta potential of alumina suspension with respect to titania sol addition.

reported on alumina-coated SiC shows that the isoelectric point of SiC is shifted from pH 4 to pH 8 after coating with alumina [19]. The shift in the isoelectric point is explained on the basis of specific adsorption of alumina on SiC surfaces. In another study, the isoelectric point of α-Al_2O_3 was found to shift from pH 7.5 to pH 2.2 due to the specific adsorption of poly acrylic acid (PAA) [20]. In the present work, alumina suspension was prepared at pH 3.0 leading to a zeta potential value of +60 mV. Similarly titania sol prepared at pH 3.0 has a zeta potential value of +2.9 mV. Therefore, the titania nanoparticles produced by the hydrolysis of the titanium tetra chloride solution will have a spontaneous tendency to self-assemble on the surface of the alumina particles by heterocoagulation. Single layer of titania is sufficient to alter the electrokinetic behaviour of surface of alumina particles, which may indicate the uniformity of titania coating achieved in the present procedure.

The process of coating of titania on alumina was monitored by the addition of 5–25 mL titania sols to alumina suspension separately and measuring the zeta potential of the suspension. The corresponding results are shown in Fig. 2. The initial pH was 2.0 and the zeta potential is +22 mV. The addition of titania sol from 5 to 25 mL causes a dramatic decrease of zeta potential values from +22.0 to −10 mV, while the pH value of the alumina suspension increased from 2.0 to 2.4. The sharp decrease in zeta potential indicated that titania particle had already got adsorbed on to the surface of alumina particle and is progressive with increasing titania concentration as shown in Fig. 2.

The XRD patterns of the as-coated and dried powder show only the peaks of alumina, meaning that the TiO_2 coating is mainly amorphous (Fig. 3). The intensity of the titania diffraction pattern was much lower than that of Al_2O_3 hence it was very hard to detect such pattern from normal XRD pattern. The 1000 °C calcined powder shows highly crystalline peaks for titania. The coating is confirmed by the results of the X-ray photoelectron spectroscopy (XPS) studies. According to literature, the highest intensity peaks of Al (2*s*) and Al (2*p*) are observed at 74.0 and 74.2 eV, respectively [21]. The results of XPS (powder calcined at 1000 °C) show that the highest intensity peaks of alumina are attenuated and hence it is confirmed that a uniform coating of titania exits over alumina (Fig. 4(a)). The XPS spectrum also shows the presence of major peaks of Ti (2*p*) 458.5 eV [22].

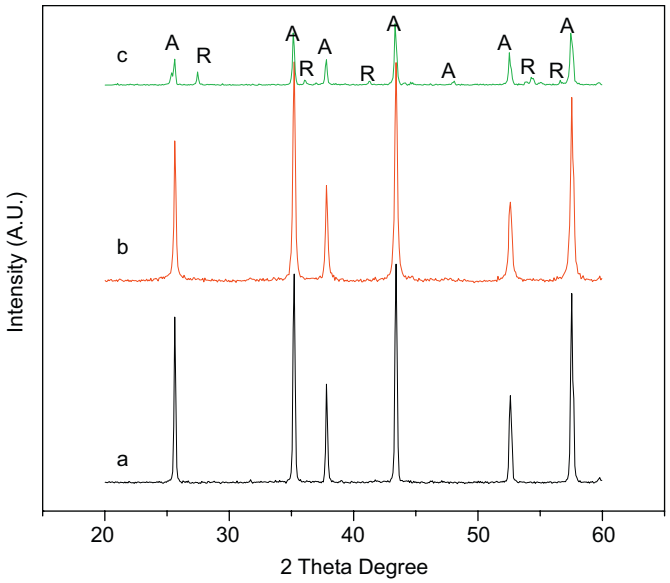

Fig. 3. X-ray diffraction pattern of (a) alumina, (b) alumina–aluminium titanate precursor dried at 80 °C, and (c) alumina–aluminium titanate precursor calcined at 1000 °C A-alumina, R-titania.

The high-resolution XPS spectra of the O (1*s*) and Ti (2*p*) are shown in Fig. 4(b) and (c), respectively. The peak of Ti (2*p*) at 458.5 eV is shifted compared to pure titania. The O (1*s*) peak of TiO_2-coated alumina particle was shown in Fig. 4(b) which indicates that the main peak of O (1*s*) consists of a main peak and a shoulder [23]. According to literature, one peak can be assigned to bulk O^{2-} and the other peak to −OH. The −OH and bulk O^{2-} peaks of the coated Al_2O_3 particle surface are assigned to $Ti(OH)_4$. The intensity of −OH is large compared to the bulk O^{2-} and this is due to the adsorbed coating film of hydrous $Ti(OH)_4$ rich in −OH [24]. The absence of alumina peak in the titania-coated alumina particle suggested that a thick coating of titania is formed on the alumina particle [25]. Therefore, only the peaks of titanium, oxygen and carbon are observed in the spectra of titania-coated alumina particle [26].

The microstructure of titania coating on alumina was observed by TEM and details are presented in Fig. 5(a). Alumina particles

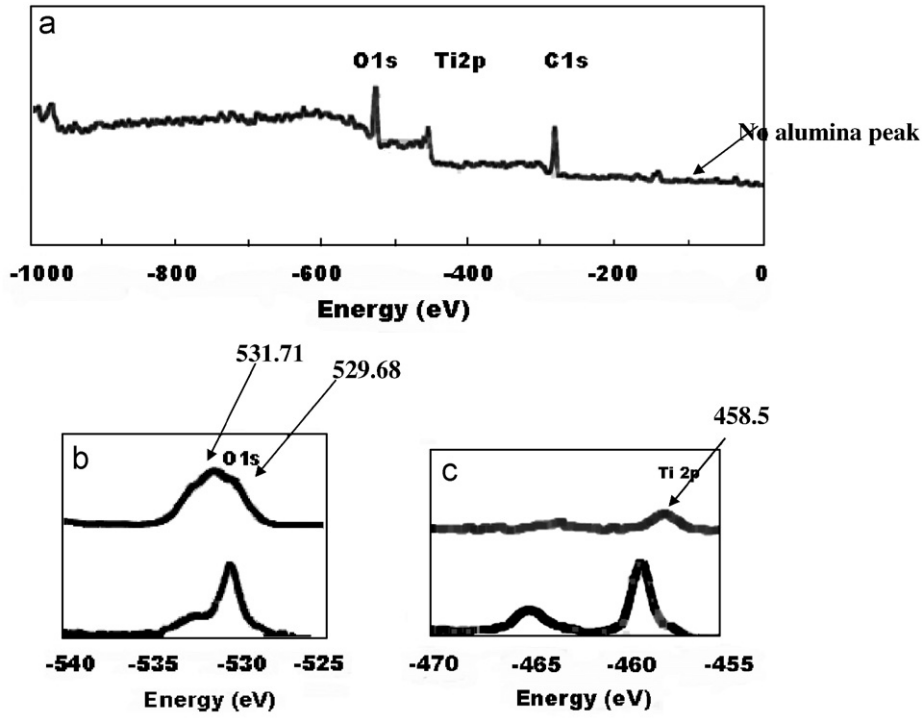

Fig. 4. (a) XPS survey of Al–20AT precursor calcined at 1000 °C. (b) High-resolution XPS spectra of the O (1*s*) of the Al–20AT precursor calcined at 1000 °C. (c) High-resolution XPS spectra of the Ti (2*p*) of the Al–20AT precursor calcined at 1000 °C.

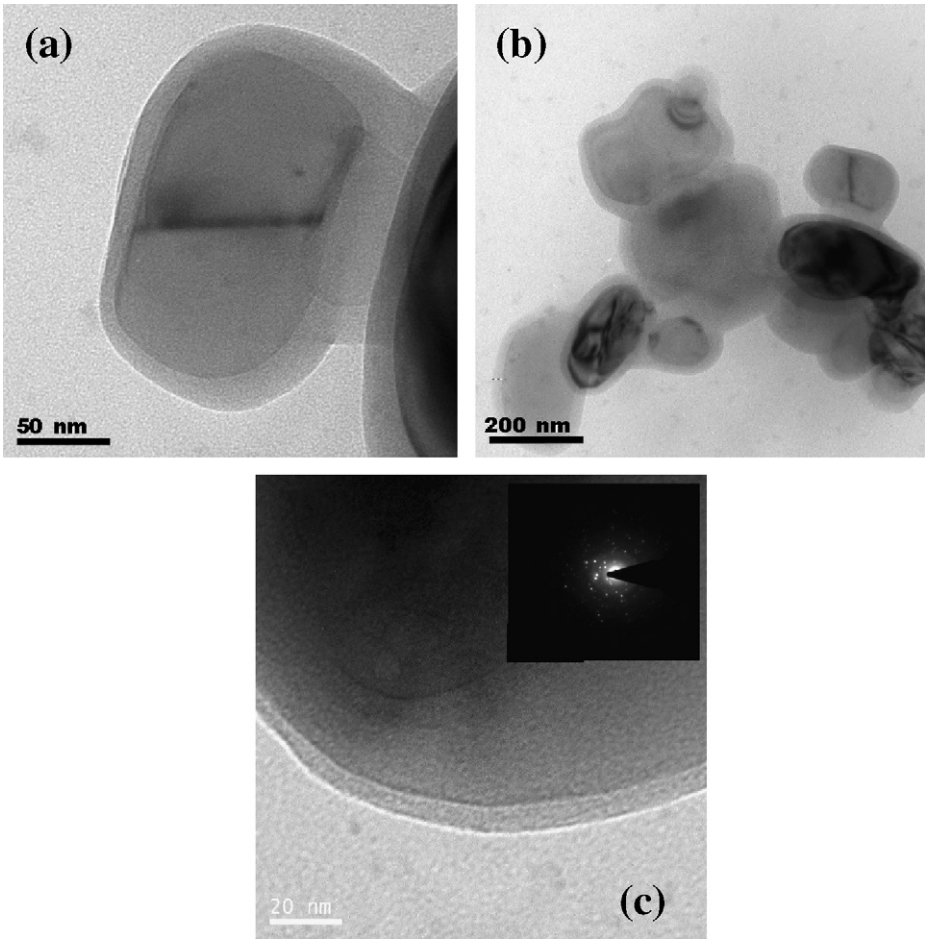

Fig. 5. (a) Typical TEM image of Al_2O_3 @ TiO_2 single particle. (b) Typical TEM image of Al_2O_3 @ TiO_2 a cluster of particles. (c) Morphology of Al_2O_3 @ TiO_2, and inset shows the corresponding SAED pattern.

are fully covered by titania with an average thickness of almost 24 nm. The TiO_2-coated alumina powder calcined at 1000 °C shows the presence of a smooth layer of titania coating. In some cases, a cluster of alumina particles is uniformly coated with nano titania layers with an average coating thickness of 24 nm or sometimes titania-coated alumina particles are stacked together as is shown in Fig. 5(b). Particles even larger than 200–400 nm could be easily coated by the present approach. The coating was crystalline as shown by the SAED pattern presented in Fig. 5(c). The macroscopic driving forces responsible for the spontaneous assembly of the nanocrystals in the shell are related to the replacement of solid–liquid interfaces by solid–solid interface of lower energy. Also the entropy is increased because water and absorbed ions are removed [26]. The centre of the alumina particle is darker than their outer regions because the centre of a spherical particle is thicker [27].

Many researchers refer to electrostatic attraction in order to explain the coating of the shell-particles on a core in an aqueous medium because of opposite surface charges. Other suggested mechanisms are the heterogeneous nucleation on the core particle or ion adsorption on the core. Furthermore, Wu et al. suggested the collision of the shell-particle and core particle substrate followed by a condensation between them [28].

The particle size distribution of TiO_2-coated Al_2O_3 dried at 80 and 1000 °C is presented in the Fig. 6. The powder dried at 80 °C shows an average particle size of 340 nm with a PDI value (poly dispersity index) of 0.4, whereas 1000 °C calcined sample shows 486 nm average particle size. Al_2O_3 mechanically mixed (solid-state mixing) with TiO_2 shows higher particle size distribution. The sample at 1000 °C shows a higher particle size due to aggregation of the particle in aqueous medium compared to as dried powder.

The XRD analysis of the reference sample calcined at 1300 °C shows the presence of alumina and rutile titania phase, whereas the core–shell approach shows the presence of alumina and aluminium titanate phases (Fig. 7). This shows that the present core–shell

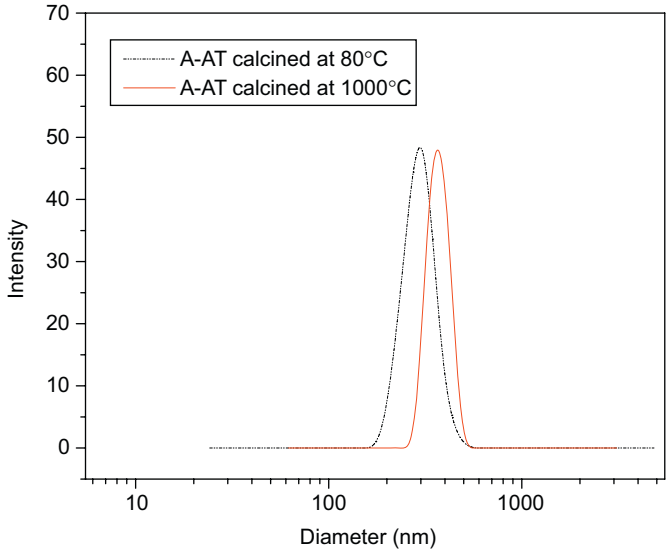

Fig. 6. Particle size of sol–gel coated Al–20AT at 80 and 1000 °C.

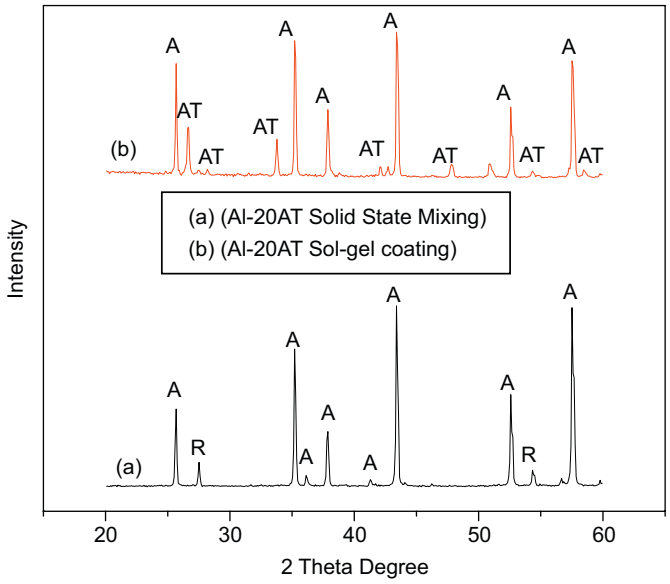

Fig. 7. XRD of Al–20AT (a) solid-state mixing and (b) sol–gel coating at 1300 °C, R-rulite titania, A-alumina, AT-aluminium titanate.

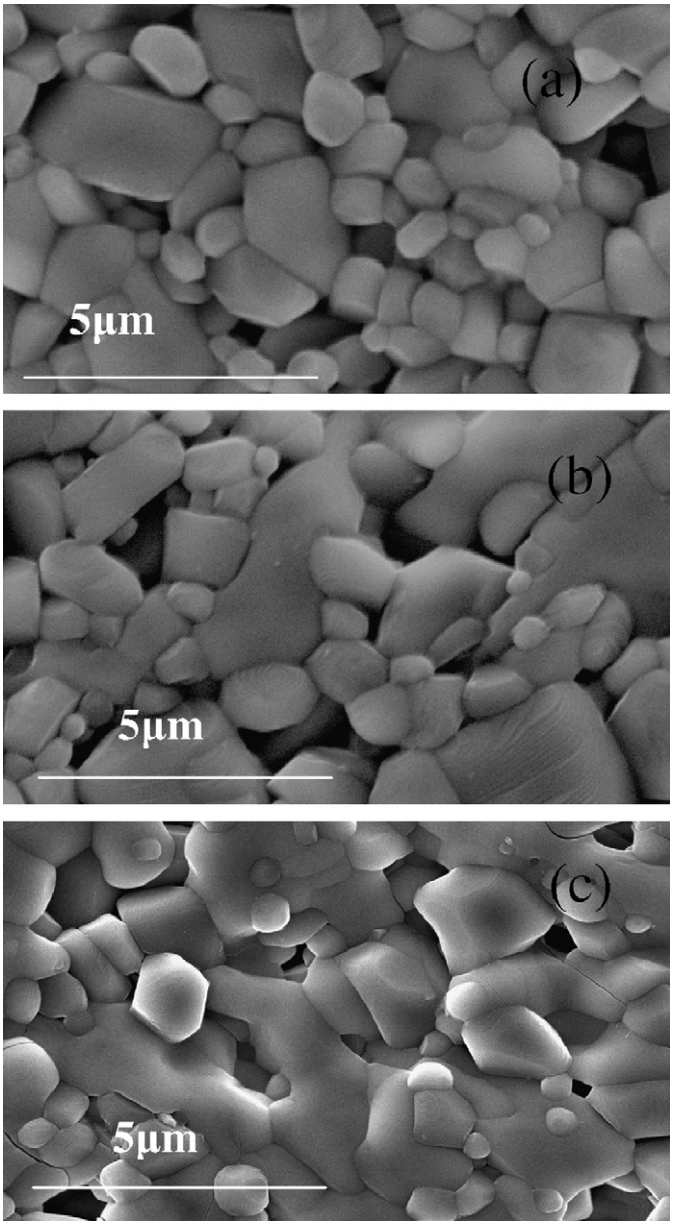

Fig. 8. Alumina–aluminium titanate composite sintered at 1350 °C: (a) Al–5AT, (b) Al–20AT, and (c) Al–50AT composite sintered at 1450 °C.

approach was effective in the low temperature formation of aluminium titanate compared to the conventional solid-state mixing route because of the faster diffusion rate due to proximity [29,30].

3.2. Sintering and microstructure development

The sintering of alumina–aluminium titanate precursor compact was carried out in the temperature range of 1350–1450 °C with 3 h soaking time. The typical sintering schedule was as follows: RT–800 °C at a rate of 3 °C min^{-1}, 800–1200 °C at a rate of 5 °C min^{-1} and then up to maximum sintering temperatures at 10 °C min^{-1}.

The green compacts of alumina–20 vol% of aluminium titanate composite precursor on subsequent heat treatment at 1300 °C resulted in higher density. However, composites with larger second phase contents (20–40 vol%) gave lower densities (95% of theoretical) [31]. The low temperature sintering is due to the faster diffusion rate in core–shell particle compared to the conventional solid-state sintering route. The average grain size of aluminium titanate and alumina is 1.5 μm and 2.0 μm, respectively. Fig. 8(a) and (b) shows SEM micrograph of sintered Al–5AT and Al–20AT composites at 1350 °C, respectively. The addition of AT to Al_2O_3 expected to control the grain growth of both alumina and aluminium titanate. On the other hand, Fig. 8(c) indicates further grain growth observed and this sample was sintered at 1450 °C. No microcracks are observed in any of the samples sintered at lower temperature indicating the absence of abnormal grain growth of AT grains. Under the present conditions of preparation, the aluminium titanate particle were preferentially distributed at the grain boundaries and this could be due to the novel approach of the pre-coated precursor. The distribution of aluminium titanate grains in the alumina matrix was confirmed by SEM–EDX analysis as shown in Fig. 9. The microstructure analysis of the composite shows that the grain size of aluminium titanate is lower than the initial particle size of alumina. The titania in the precoated alumina particles get converted to rutile at 1200 °C and get distributed at the grain boundaries of alumina which could initiate the sintering process. However aluminium titanate once formed may preclude further densification of the composite. More cohesive microstructures may be possible by a rate controlling technique in sintering.

4. Conclusion

A novel synthesis route based on core–shell approach for alumina–aluminium titanate composites as well as the low temperature sintering resulting in a fine-grained microstructure was reported. Formation of amorphous titania shell on alumina particles kept in stoke suspension was achieved at high zeta potential value of +20 mV. The formation temperature of aluminium titanate from the precursor containing Al_2O_3 and TiO_2 can be

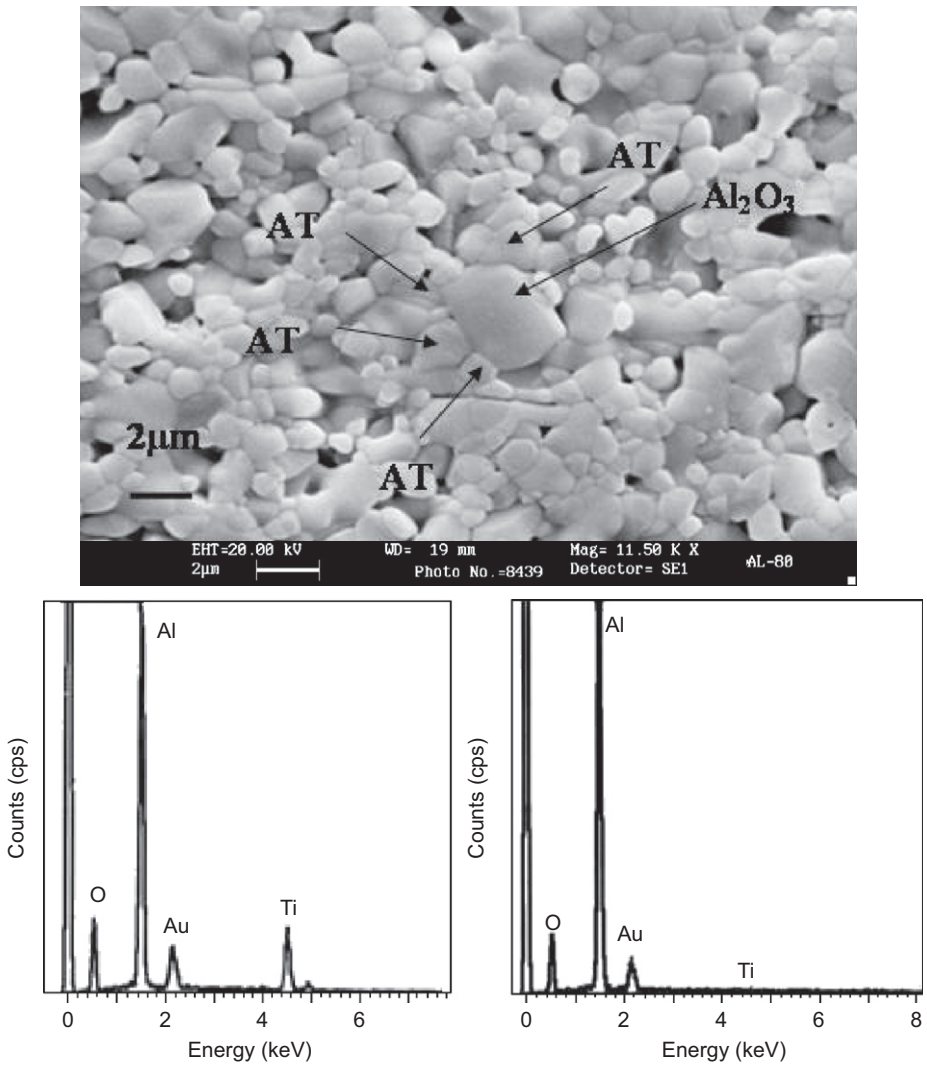

Fig. 9. Al–20AT composite sintered at 1350 °C (marked area is the spot were the EDX analysis was performed).

drastically reduced by the TiO_2-coated Al_2O_3 precursor particles compared to using a mechanical mixture of alumina and titania. The low temperature formation of aluminium titanate in the alumina matrix can be attributed to a maximum contact area between the reactants in the core–shell approach when compared to the solid-state mixing route. The present approach results in good densification without significant grain growth. The composite sintered at 1350 °C shows a sintered density of 98% with an average grain size of 2 μm and 1.5 μm for alumina and aluminium titanate, respectively.

Acknowledgments

The authors acknowledge the members of Materials and Minerals Division for discussion on the results obtained. One of the authors, M. Jayasankar, is grateful to Department of Science and Technology (DST) and Council of Scientific and Industrial Research (CSIR), India, for providing financial support and research fellowship, respectively.

References

[1] H.A.J. Thomas, R. Stevens, Br. Ceram. Trans. J. 88 (1989) 144–151.
[2] J.J. Clevland, R.C. Bradt, J. Am. Ceram. Soc. 61 (1978) 478–481.
[3] P. Innocenzi, A. Martucci, L. Armelao, S. Licoccia, M. Luisa Di Vona, E. Traversa, Chem. Mater. 12 (2000) 517–524.
[4] B. Freudenberg, A. Mocellin, J. Am. Ceram. Soc. 70 (1987) 33–38.
[5] Y. Ohya, Z. Nakagawa, J. Am. Ceram. Soc. 70 (1987) C184–C186.
[6] T. Matsudaira, Y. Kuzushima, S. Kitaoka, H. Awaji, D. Yokoe, J. Ceram. Soc. Jpn. (Suppl. 112–1, Pacrim5 Special Issue) (2004) S327–S332.
[7] M. Taguchi, Adv. Ceram. Mater. 3 (1987) 1735–1762.
[8] N.P. Padture, S.J. Bermison, H.M. Chan, J. Am. Ceram. Soc. 76 (1993) 2312–2320.
[9] M. Andrianainarivelo, R.J.P. Corriu, D. Leclercq, P.H. Mutin, A. Vioux, Chem. Mater. 9 (1997) 1098–1102.
[10] Y. Yang, O. Chen, A. Angerhofer, Y.C. Cao, J. Am. Chem. Soc. 128 (2006) 12428–12429.
[11] Y.F. Tang, L. Feng, Y. Chen, A.D. Li, Adv. Eng. Mater. 6 (2004) 69–71.
[12] J.-Y. Lee, J.-H. Lee, S.-H. Hong, Y.K. Lee, J.-Y. Choi, Adv. Mater. 15 (2003) 1655–1658.
[13] Q. Liu, Z. Xu, J.A. Finch, R. Egerton, Chem. Mater. 10 (1998) 3936–3940.
[14] X.-C. Guo, P. Dong, Langmuir 15 (1999) 5535–5540.
[15] D. Ma, T. Veres, L. Clime, F. Normandin, J. Guan, D. Kingston, B. Simard, J. Phys. Chem. C 111 (2007) 1999–2007.
[16] C.Y. Yang, W.Y. Shih, W.H. Ship, J. Am. Ceram. Soc. 84 (2001) 2834–2840.
[17] M. Jayasankar, S. Ananthakumar, P. Mukundan, K.G.K. Warrier, Mater. Lett. 61 (2007) 790–793.
[18] M. Jayasankar, S. Ananthakumar, P. Mukundan, K.G.K. Warrier, J. Am. Ceram. Soc. 90 (2007) 3091–3094.
[19] U.S. Hareesh, M. Sternitzke, R. Janssen, N. Claussen, K.G.K. Warrier, J. Am. Ceram. Soc. 84 (2004) 1024–1030.
[20] J. Sun, L. Gao, W. Li, Chem. Mater. 14 (2002) 5169–5172.
[21] M. Casarin, D. Falcomer, A. Glisenti, A. Vittadini, Inorg. Chem. 42 (2003) 436–445.
[22] C.D. Wagner, W.M. Riggs, L.E. Davis, J.F. Moulder, G.E. Muilenberg, Handbook of X-ray Photoelectron spectroscopy, Perkin-Elmer Corporation, Eden Prairie, MN, 1979.
[23] X.C. Guo, P. Dong, Langmuir 15 (1999) 5535–5540.
[24] R. Sanjnes, H. Tang, H. Berger, F. Gozzo, G. Margaritnondo, F. Leavy, J. Appl. Phys. 75 (1994) 2945–2951.
[25] G. Wang, A. Harrison, J. Colloid Interface Sci. 217 (1999) 203–207.
[26] H.-X. Wu, T.-J. Wang, Yong Jin, Ind. Eng. Chem. Res. 45 (2006) 5274–5278.
[27] L.F. Hakim, J.A. McCormick, G.D. Zhan, A.W. Weimer, P. Li, S.M. Geroge, J. Am. Ceram. Soc. 89 (2006) 3070–3075.
[28] H.-X. Wu, T.-J. Wang, Yong Jin, Ind. Eng. Chem. Res. 45 (2006) 1337–1342.
[29] M.T. Baucaglia, V. Bauscaglia, R. Alessuo, Chem. Mater. 19 (2007) 711–718.
[30] L.A. Stanciu, J.R. Groza, A. Jitianu, M. Zaharescu, Mater. Manuf. Process. 19 (2004) 641–650.
[31] H.M. Okamura, E.A. Barringer, H.K. Bowen, J. Mater. Sci. 24 (1989) 1867–1880.